Proper motion of Cygnus loop filaments

Nikolina Milanović[1], Milica Vučetić[1], Dušan Onić[1], John Raymond[2], Dejan Urošević[1]

[1]Department of Astronomy, Faculty of Mathematics, University of Belgrade, Serbia
[2]Smithsonian Astrophysical Observatory, Harvard University, USA

Abstract: In this poster we determine the shock velocities in the Cygnus Loop supernova remnant, using proper motions of the filaments in the remnant. The proper motions were measured by comparing the Hα images of the remnant observed in two epochs: in 1993 (obtained at Kitt Peak National Observatory), and in 2018 (obtained at National Astronomical Obsevatory Rozhen, Bulgaria). Then the shock velocities were derived using the most recent distance estimate of Cygnus Loop (735 ± 25 pc), based on Gaia DR2 parallax measurements of several stars (Fesen et al., 2018). The velocities of both nonradiative and radiative filaments were obtained and compared. Radiative filaments were selected as those that are visible in [SII] images of the remnant.

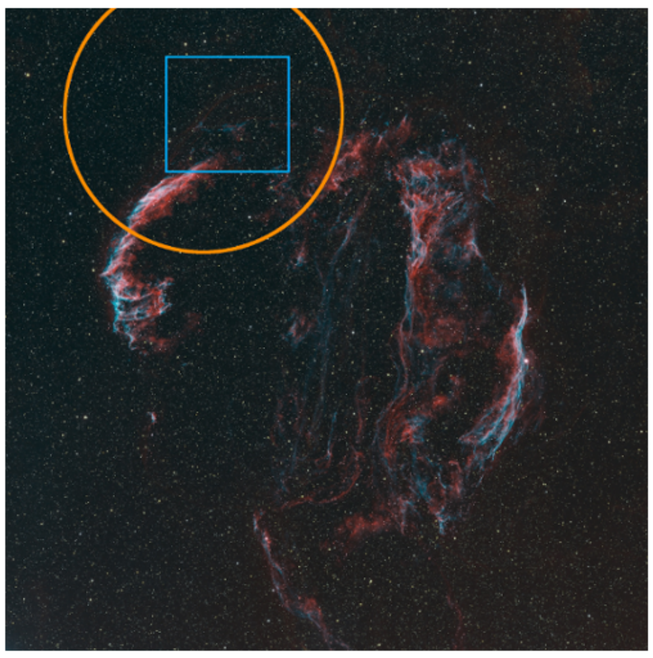

Figure 1. Cygnus loop (red: Hα, blue: [OIII], green: [SII]; Credits: Martin Pugh). Orange region shows the location of the 1993 data, and blue one of the 2018 data that we use.

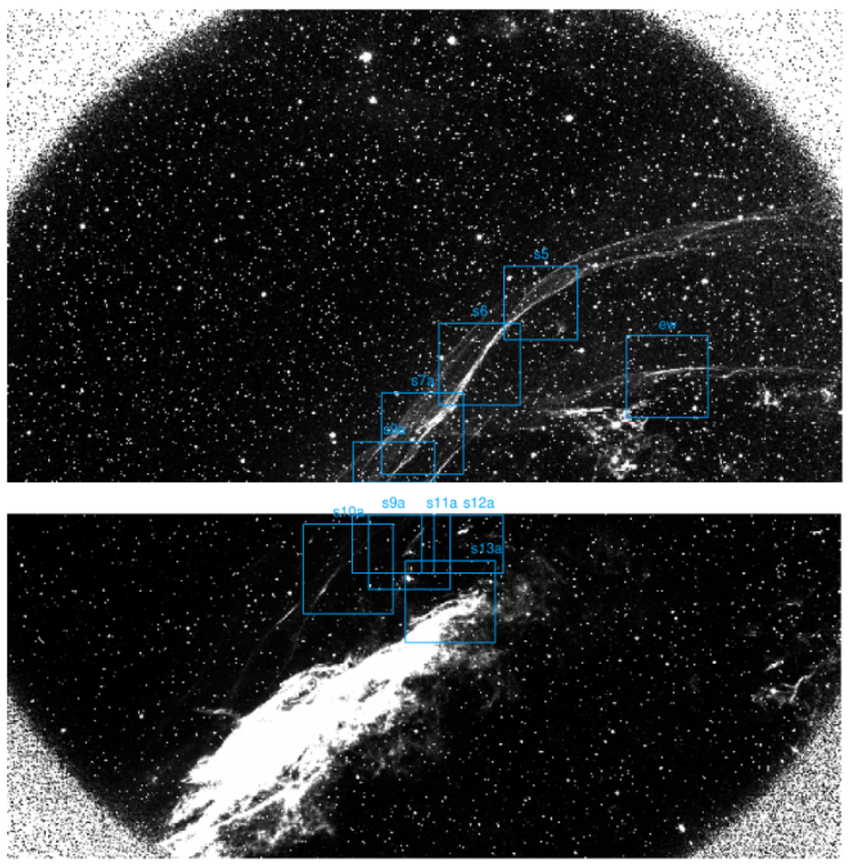

Figure 2. The observation of Cygnus loop in Hα filter from 1993, observed with Burrell Schmidt telescope (0.9 m), KPNO (private comunication with Robert A. Fesen). The image scale is 2.0268"/px. Blue regions represent the fields that were observed in Hα and [SII] filters in 2018 by our group, using 2 m telescope at Rozhen NAO, Bulgaria. The scale for those images is 0.176"/px, while the seeing was 1.2"-1.8".

Shock waves in SNRs evolve from being non-radiative to radiative. Radiative shocks are expected to have lower velocities, since they are supposed to be evolutionary old. A single supernova remnant (like Cygnus loop, Figure 1) can be complicated in structure and have both non-radiative and radiative shocks, depending on the environment in which it expands. We can distinguish radiative from non-radiative shocks by taking observations in Hα and [SII] filters, where non-radiative shocks would be visible only in Hα, while radiative shock would be visible in both filters.

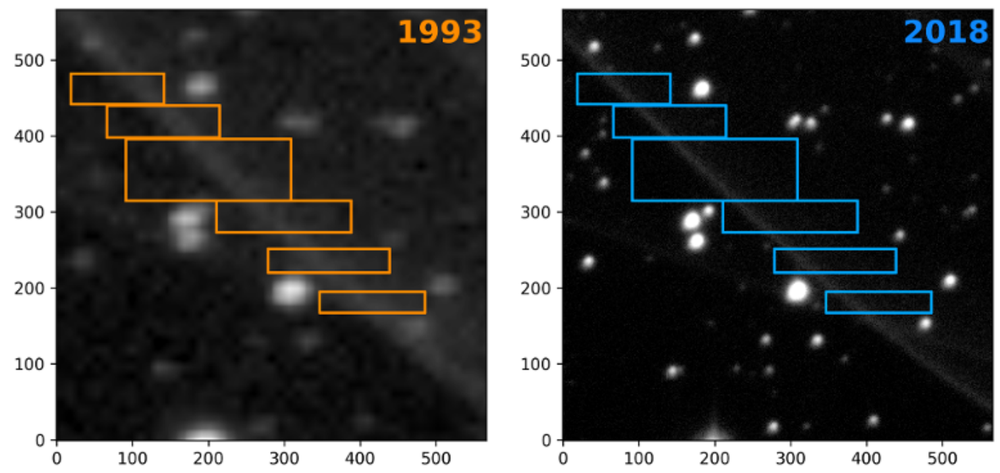

Figure 3. An example of nearly linear filament in both of the epochs, with selected regions without stars.

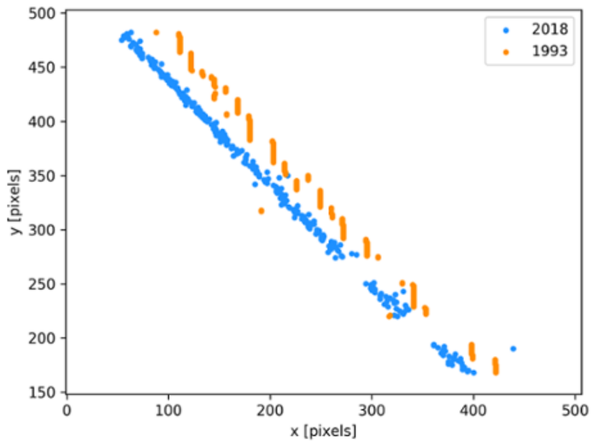

Figure 4. Extracted maximums of intensity in selected rows for the filament from Figure 3.

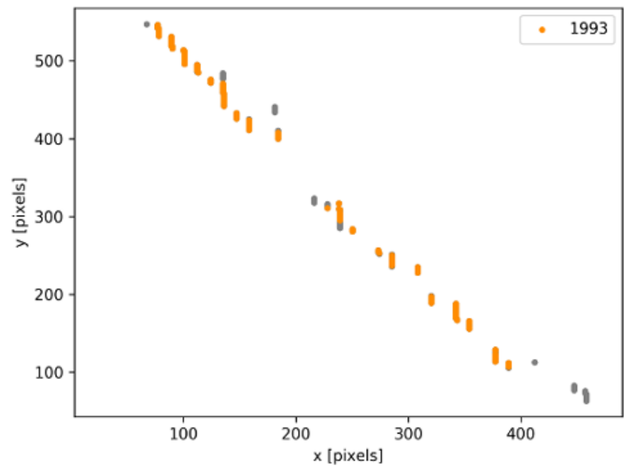

Figure 5. Example of the extracted maximums for more dispersed filament, where the dots in grey are the ones that were itteratively discarded using sigma clipping.

Proper motion measurement process:

0. Interpolating the 1993 images linearly (2.0268" → 0.176") and overlapping them with 2018 images.
1. Finding a nearly linear filament. → Figure 3.
2. Selecting suitable regions (no stars, no other filaments, well covered movement). → Figure 3.
3. Finding maximums of the intensity (for each row in the selected regions). → Figure 4.

3 ×
4. Fitting the filament with a linear function and sigma clipping (±2σ). → Figure 5.

10000 ×
5. Random resampling those rows.
6. Finding mean proper motion (mean values of motions for each row).
7. Fitting the filament with a linear funtion and finding its slope.
8. Projecting mean proper motion to the direction perpendicular to the filament.

Table 1. Measured filaments and comparison with Salvesen et al. (2009) and Medina et al. (2014).

This work					Salvesen et al. (2009)			Medina et al. (2014)	
name	RA	DEC	pm ["]	v [km/s]	name	v [km/s]	v_n [km/s]	name	v [km/s]
ew i1	20:53:40.38	32:14:14.53	2.49 ± 0.10	350 ± 20					
ew i2	20:53:27.21	32:14:22.10	2.36 ± 0.06	330 ± 20					
s5 i1	20:54:28.36	32:20:13.47	3.89 ± 0.10	540 ± 20					
s5 i2	20:54:20.15	32:21:57.44	4.22 ± 0.07	590 ± 20					
s5 i3-2	20:54:13.65	32:22:25.90	3.61 ± 0.06	500 ± 20				NFil (w/o NFili)	429 ± 22
s6 i1	20:54:51.03	32:17:21.87	3.38 ± 0.09	470 ± 20					
s6 i2-1	20:54:35.87	32:17:42.67	1.34 ± 0.04	190 ± 10					
s6 i2-2	20:54:35.87	32:17:42.67	2.06 ± 0.05	290 ± 10				FUSEA	428 ± 7
s6 i3	20:54:44.56	32:15:47.93	3.29 ± 0.05	460 ± 20	6	333	384	S6 (w/o S6e)	391 ± 3
								COS 1	405 ± 8
s6 i4	20:54:51.33	32:14:11.08	3.30 ± 0.06	460 ± 20					
s7a i1	20:54:57.70	32:08:11.42	2.57 ± 0.10	360 ± 20					
s7a i4	20:55:13.57	32:08:26.66	3.91 ± 0.10	540 ± 20					
s7a i5	20:55:11.37	32:12:11.02	2.34 ± 0.20	320 ± 30					
s9a i1	20:55:28.73	32:07:55.05	2.33 ± 0.07	320 ± 20					
s9a i3	20:55:19.61	32:06:56.97	1.99 ± 0.07	280 ± 20	9	294	339	$S89_{ON}$ (w/o S8a)	457 ± 22
								$S89_{OFF}$ (w/o S8a)	382 ± 6
s9a i4	20:55:14.05	32:08:19.48	3.90 ± 0.08	540 ± 20					
s10a i1	20:55:34.62	32:01:44.56	1.95 ± 0.04	270 ± 10	10	279	322	S10	342 ± 46
s10a i2	20:55:44.76	31:59:49.90	1.87 ± 0.05	260 ± 10	11	254	293		
s10a i3	20:55:42.79	32:02:13.79	3.47 ± 0.10	480 ± 20					
s11a i2-1	20:55:15.11	32:03:31.53	2.17 ± 0.06	300 ± 20					
s11a i2-2	20:55:15.11	32:03:31.53	1.65 ± 0.05	230 ± 10					
s11a i3-1	20:55:19.70	32:02:37.78	1.90 ± 0.17	260 ± 30					
s11a i3-2	20:55:19.70	32:02:37.78	1.67 ± 0.12	230 ± 20					
s11a i4	20:55:18.53	32:00:38.91	1.58 ± 0.06	220 ± 10					
s13a i1	20:55:12.37	31:55:57.79	0.82 ± 0.05	110 ± 10					
s13a i2-1	20:54:53.09	31:57:59.17	0.89 ± 0.04	120 ± 10					
s13a i2-2	20:54:53.09	31:57:59.17	0.79 ± 0.10	110 ± 20					

Summary

Proper motions and velocities were obtained for 27 nearly linear filaments (Table 1), three of which were radiative (s13a). Some of our positions of measurement overlap with the positions in Salvesen et al. (2009) and Medina et al. (2014), so the values of velocities were compared for those. Upper limits on the shock velocities in SNRs can be combined with the post-shock temperatures, to obtain upper limits on the ratio of cosmic ray to gas pressure behind the shocks. That is important for assessing the efficiency of the energy dissipated by the SNR into accelerating cosmic rays (Medina et al., 2014).

References

Fesen, R., Weil, K., Cisneros, I., Blair, W. and Raymond, J. (2018). The Cygnus Loop's distance, properties, and environment driven morphology. MNRAS, 481(2), pp.1786-1798.

Medina, A., Raymond, J., Edgar, R., Caldwell, N., Fesen, R. and Milisavljevic, D. (2014). ELECTRON-ION EQUILIBRIUM AND SHOCK PRECURSORS IN THE NORTHEAST LIMB OF THE CYGNUS LOOP. ApJ, 791(1), p.30.

Salvesen, G., Raymond, J. and Edgar, R. (2009). SHOCK SPEED, COSMIC RAY PRESSURE, AND GAS TEMPERATURE IN THE CYGNUS LOOP. ApJ, 702(1), pp.327-339.